



## Folding endurance of continuous silicon carbide fibres: A comparative study

Qianhe Li, Yantao Gao\*, Md All Amin Newton, Zan Lu, Xue Yang, Binjie Xin

*School of Textiles and Fashion, Shanghai University of Engineering Science, Shanghai 201620, China*

Received 18 October 2023; Received in revised form 10 January 2024; Accepted 11 February 2024

### Abstract

*The limited folding resistance of continuous silicon carbide (SiC) fibres hinders their application as flexible, foldable materials. With this objective in mind, the folding endurance and damage properties of the second (2<sup>nd</sup>) and third (3<sup>rd</sup>) generation continuous SiC fibre tows were investigated through repeated folding tests, optical microscope observation and tensile tests. These SiC fibre tows were disassembled from two-dimensional (2D) SiC fibre braided fabrics with varying braiding angles. The braiding process can alleviate the force on fibre tows during the textile forming process. The investigation of damage mechanisms and analysis of force conditions are instrumental in optimizing structural parameters. The research findings suggested that, in comparison to the 3<sup>rd</sup> generation continuous SiC fibres, the 2<sup>nd</sup> generation SiC fibre tows demonstrated higher resistance to repeated folding. In contrast, the 2<sup>nd</sup> generation fabrics exhibited slightly lower folding endurance values. After repeated folding, the SiC fibre tows in fabrics showed the highest strength losses near the braiding angle of 37.8° to 38.3°. In comparison, the SiC fibre fabric demonstrated the lowest folding endurance values (approximately 760 times) near the braiding angle of 41° to 42°. Considering factors such as folding endurance value, the strength loss rate of fibre tows and fabric strength loss rate, it can be concluded that SiC fibres in fabrics with large braiding angles exhibit optimal performance in terms of folding endurance.*

**Keywords:** SiC fibre, mechanical properties, failure analysis, folding endurance

### I. Introduction

The atmospheric entry systems of aerospace vehicles primarily focus on inflatable structures and foldable mechanisms, with flexible thermal protection materials used for the outer layers of inflatable structures and umbrella-like skirt parts of folding mechanisms [1–8]. In extreme environments such as extreme cold, heat and space radiation, thermal protection materials must possess excellent properties, including high and low-temperature resistance, ageing resistance, oxidation resistance and dimensional stability. Continuous silicon carbide (SiC) fibres precisely meet these performance requirements. However, to utilize SiC fibres to fabricate flexible foldable and deployable thermal protection materials, it is imperative to investigate their characteristics, such as poor toughness, limited folding endurance and susceptibility to damage.

The most representative high-temperature resistant

fibre is Nextel ceramic oxide continuous fibre developed by the American 3M Company [9,10]. The heat-resistant layers of the thermal protection system (TPS) in NASA's High-Energy Atmospheric Reentry Test (HEART) vehicle consist of fabrics made from aluminium borosilicate fibre (3M™ Nextel™ 440 BF20), and the fabrics can still maintain high mechanical properties, flexibility and structural integrity even at 1370 °C [11,12]. The Deployable Self-Regulating Centrifugally-Stiffened Decelerator (DESCENT), proposed by the Harbin Institute of Technology, featured a flexible conical shell constructed from ceramic fabric based on an origami pattern; compared to NASA's HEART, DESCENT exhibited a superior lightweight and flexible size design, eliminating the need for insulation blankets or gas barriers [13–15]. Zhang *et al.* [16] prepared a high emissivity double-layer coating with SiC and ZrO<sub>2</sub> as emittance agents on the surface of flexible aluminium silicate fibre fabrics, effectively enhancing the fibre fabrics' tensile strength and thermal insulation performance. It can be seen that the current re-

\*Corresponding authors: tel: +86 18217155467,  
e-mail: [gaoyantao@sues.edu.cn](mailto:gaoyantao@sues.edu.cn)

search predominantly employs aluminium borosilicate fibre, quartz fibre and high silica fibre for fabricating flexible ceramic thermal protection materials. In contrast, SiC fibres find more appropriate use as coating materials.

The research on SiC fibres has undergone three generations of development, and the key is to reduce the contents of impurity oxygen and free carbon in SiC fibres while enhancing their operational temperature. In other words, the primary distinctions among various generations of SiC fibres lie in their compositional structure and temperature resistance. The near-stoichiometric composition and high crystalline structure result in exceptional properties, including elastic modulus, high-temperature resistance, creep resistance, and oxidation resistance of SiC fibres. The second (2<sup>nd</sup>) generation SiC fibre exhibits high carbon content and low oxygen content, while the third (3<sup>rd</sup>) generation SiC fibre features low carbon and oxygen levels. Currently, researchers primarily investigate the microstructure, mechanical properties, high-temperature resistance, oxidation resistance, dimensional stability, wet oxidation behaviour, microwave absorption properties and other aspects of SiC fibres under diverse environmental conditions [17–30]. The National University of Defense Technology has successfully developed various categories of continuous SiC fibres, including KD-I, KD-II, KD-S and KD-SA types, with comprehensive performance that either meets or approaches the level of similar international products [31–35]. Xiamen University has achieved the 2<sup>nd</sup> and 3<sup>rd</sup> generation continuous SiC fibres through electron beam radiation crosslinking and hydrogenation decarburization [36–38].

The application researches of SiC fibres primarily focuses on ceramic composite materials, while their use in flexible and foldable materials research is limited. Due to technical confidentiality, only a few reports have mentioned utilizing SiC fibre fabrics as flexible thermal protection materials. According to the standard GB/T 457-8 [39], “folding endurance” refers to the logarithm (base 10) of the number of sample fractures occurring under standardized tension conditions. The term “folding endurance” in this study specifically refers to the material’s capacity to endure repeated folding. Previously, we studied the folding endurance of the 3<sup>rd</sup> generation SiC fibres and their fabrics [42]. However, on the basis of our previous research, this paper paid special attention to the 2<sup>nd</sup> and 3<sup>rd</sup> generation SiC fibres and their fabrics, and deeply explored the differences in folding endurance of different SiC fibres to inform and enhance the optimization of fabric design and performance. This study investigated the folding endurance and damage characteristics of the 2<sup>nd</sup> and 3<sup>rd</sup> generation continuous SiC fibre tows and their fabrics through repeated folding tests, optical microscope observation and tensile tests. By manipulating factors such as braiding angle, number of folds and folding angle, the relationships between SiC fibres’ folding damage and these

factors during the braided forming process and repeated folding process were examined.

In this article, various types of continuous SiC fibres were utilized to prepare two-dimensional (2D) biaxial braided fabrics with different braiding angles, and the geometric parameters of these fabrics were measured. Subsequently, the repeated folding tests and folding life tests were conducted under various folding conditions on the SiC fibre fabrics, and the damage morphologies at the fabric folding lines were characterized using a high-definition charge-coupled device (CCD) optical microscope. Furthermore, the tensile properties of SiC fibre tows and their fabrics were investigated through tensile tests, and the strength loss rates were calculated to assess the folding damage extent of SiC fibre tows and their textiles. This study should establish a foundation for future applications of SiC fibres in space flexible deployable and foldable structures.

## II. Experimental

### 2.1. Preparation of SiC fibre fabrics

The 2<sup>nd</sup> generation SiC fibres used in this article are ShinColon-II continuous SiC ceramic fibres (linear density is 310 tex, volume density is 2.7 g/cm<sup>3</sup>, tow is 1000 pieces/bundle) produced by Ningbo Zhongxing New Material Technology Co. Ltd. The 3<sup>rd</sup> generation SiC fibres are Cansas-3303 continuous SiC fibres [42] (line density is 182 tex, volume density is 3.1 g/cm<sup>3</sup>, tow is 500 pieces/bundle) produced by Fujian Leadasia New Material Co. Ltd. Based on the regular braid (2/2 repeat) structure, a self-built 32-spindles vertical 2D braiding machine [42] was used to prepare 2D biaxial SiC fibre braided fabrics (Fig. 1). SiC fibre fabrics with different

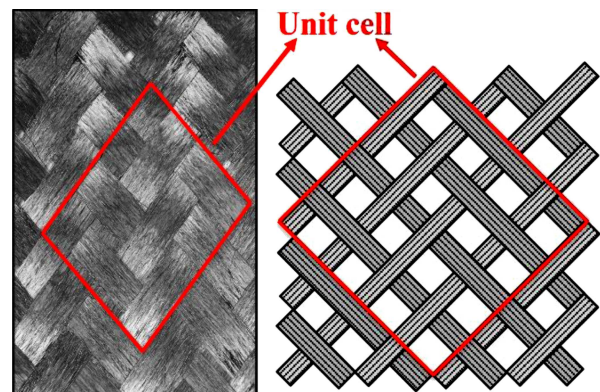


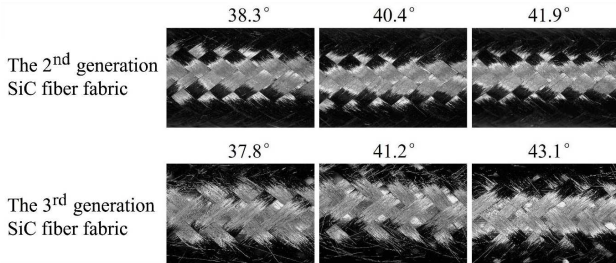
Figure 1. Fabricated SiC fibre fabric and regular braid pattern with a 2/2 repetition configuration

Table 1. Braiding process parameters of SiC fibre fabrics

Plan	Number of yarns i the bobbin	Braiding speed [r/min]	Drafting speed [mm/min]
1	1	6.5	200
2	1	7.5	200
3	1	8.5	200

**Table 2. Measured geometric parameters of SiC fibre fabrics**

Parameter	The 2 <sup>nd</sup> generation SiC fibre fabric			The 3 <sup>rd</sup> generation SiC fibre fabric [42]		
Braiding speed [r/min]	6.5	7.5	8.5	6.5	7.5	8.5
Braiding angle [°]	38.3	40.4	41.9	37.8	41.2	43.1
Thickness [mm]	0.365	0.357	0.382	0.388	0.385	0.399
Mass per unit area [g/m <sup>2</sup> ]	181.25	183.90	188.37	268.40	279.36	291.18



**Figure 2. SiC fibre fabrics with different braiding angles obtained by using different braiding speeds**

braiding angles were designed by changing the braiding and drafting speeds. The braiding process parameters are shown in Table 1.

### 2.2. Measurement of braiding geometric parameters

The braiding angle is the angle between the yarn direction and the axial braiding direction, and the surfaces of braided fabrics were observed with an optical microscope to calculate the average braiding angles. The SiC fibre fabric thicknesses were measured by a YG141LA digital fabric thickness gauge. The fabric qualities were measured by a LE104E electronic balance to calculate the masses per unit area. Samples with three different braiding angles were obtained by using different braiding speeds as shown in Fig. 2 and corresponding geometric parameters are given in Table 2.

### 2.3. Characterization

SiC fibres’ folding endurance is related to the service life and mechanical properties of the flexible, foldable material made from them. This section mainly introduces the repeated folding test, optical microscope damage characterization of different kinds of SiC fibre braided fabrics and the tensile test of SiC fibre tows and fabrics before and after folding.

#### Folding test

Repeated folding tests and folding life tests (Fig. 3) of the SiC fibre braided fabrics were carried out with

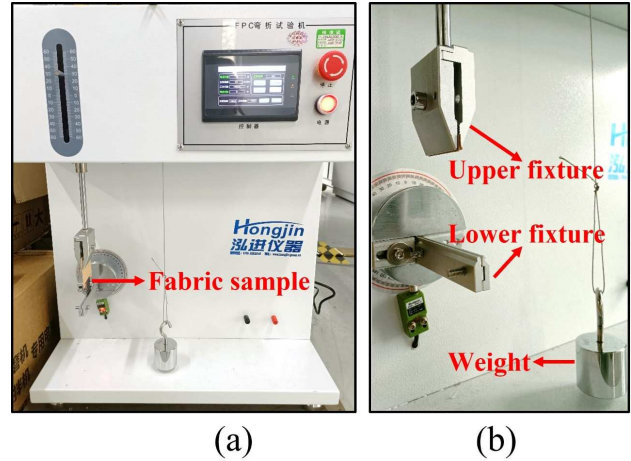


**Figure 3. Folding test process: a) reverse bend tester utilized in the folding test, b) an overview of the test device employed for assessing folding characteristics**

an HXQ-FPC reverse bend tester according to GB/T 457-2008 standard [39]. During the test, the lower fixture was rotated in a reciprocating motion, and the *R*-angle diameter of the folding fixture was 1.0 mm. All fabric samples were 50 mm long, the folding line was along the axial braiding direction and the folding speed was 50 times/min. Since the fabric sample lengths were shorter than the distance between the upper and lower fixtures, the fabrics were pasted with cardboard to extend the samples. The test parameters are summarized in Table 3. If the folding motions were continued until the fabric samples were broken (marked by the automatic stop of the tester), the operating interface of the folding tester would display the folding endurance value.

#### Tensile test

*Fibre tows tensile test* - The tensile properties of the 2<sup>nd</sup> and 3<sup>rd</sup> generation SiC fibre tows were tested according to GB/T 34520.4-2017 standard [40] by XS(08)F2 series electronic fabric strength machine [42]. The load was applied along the axial direction of the fibre tows with the tensile speed of 20 mm/min while the

**Table 3. Folding test parameters of SiC fibre fabrics**

Plan	Number of folds	Folding angle [°]	Distance between fixtures [mm]	Tension [N]
1	0	No folding	Nothing	Nothing
2	100	+135°, -0°	60	4.91
3	25	+180°, -0°	60	4.91
4	50	+180°, -0°	60	4.91
5	100	+180°, -0°	60	4.91
6	Folding until fracture	+180°, -0°	60	4.91
7	Folding until fracture	+180°, -180°	60	4.91



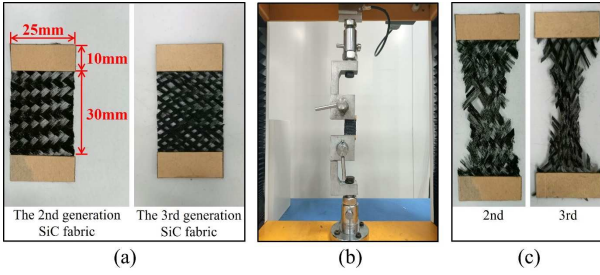


**Figure 4. Fabric tensile test: a) fabric sample, b) visual representation of the tensile test in progress and c) close-up view of the fabric at the point of tensile fracture**

tensile samples had the test gauge length of 40 mm [42]. The average values of 8 groups of effective test results were taken. The tensile forces of the original SiC fibre tows were obtained, and that of the tows disassembled from SiC fibre braided fabrics before and after folding. To evaluate the damage degree of SiC fibre tows during braiding and folding, the yarn force loss rate (*FLR*) was calculated by the following formula:

$$FLR = \frac{FO - FA}{FO} \times 100 \quad (1)$$

where *FO* is the breaking force of the original SiC fibre tows and *FA* is the breaking force of the fibre tows disassembled from SiC fabrics.

*Fabric tensile test* - XS(08)F2 series electronic fabric strength machine was used to carry out tensile tests on the braided fabrics before and after folding, including the 2<sup>nd</sup> and 3<sup>rd</sup> generation SiC fibre fabrics, according to GB/T 33613-2017 standard [41]. The load was applied along the radial braiding direction, the tensile speed was 20 mm/min and the test gauge length was 30 mm (Fig. 4a). The average values of the effective test results of 4 groups were taken. Similarly, to evaluate the damage degree of SiC fibre braided fabrics, the average strengths of the fabrics before and after folding were used to calculate the fabric force loss rate.

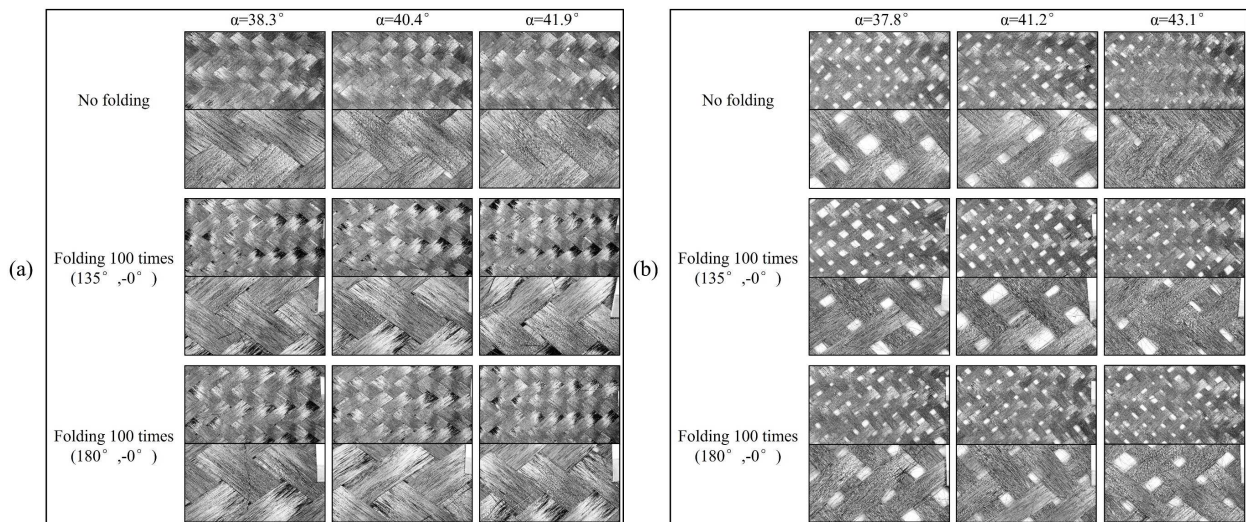
### III. Results and discussion

In order to optimize the structural parameters and resistance to bending and folding of SiC fibre braided fabrics, the folding endurance and damage mechanisms of the 2<sup>nd</sup> and 3<sup>rd</sup> generation SiC fibres and their fabrics were compared and analysed under the conditions of different braiding angles, number of folds and folding angles.

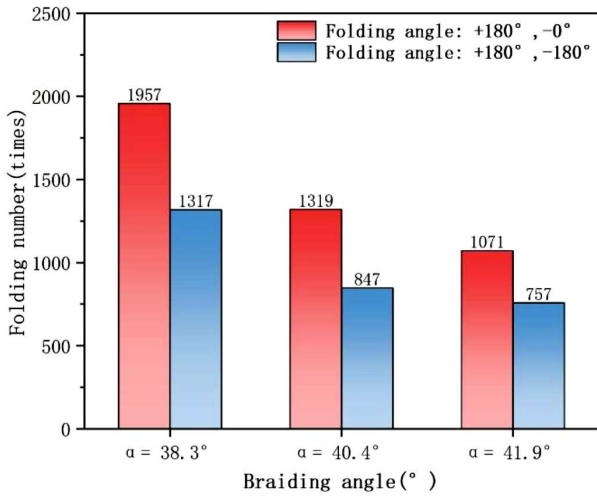
#### 3.1. Folding test results and analysis

Figure 5 indicates the surface morphologies of the 2<sup>nd</sup> and 3<sup>rd</sup> generation SiC fibre braided fabrics under different folding conditions observed by the optical microscope. The surfaces of fabrics were relatively flat and the arrangements of fibre tows were relatively orderly before folding. After folding, the surfaces of fabrics showed apparent abrasion phenomena such as fuzzing and snagging, accompanied by some local filament-breaking signs. Moreover, the phenomenon of disordered arrangements of these fibre tows became increasingly prominent with the increase in the number of folds and folding angles, leading to deformation and wear in the fabrics and ultimately resulting in damage propagation. Compared with the 3<sup>rd</sup> generation SiC fibre fabrics, the surface abrasions of the 2<sup>nd</sup> generation SiC fabrics were generally more subtle. Because the linear density of the 2<sup>nd</sup> generation SiC fibre tows (310 tex) was higher than that of the 3<sup>rd</sup> generation SiC fibre tows (182 tex), the 2<sup>nd</sup> generation fabrics were more compact, and the cover factors were higher than that of the 3<sup>rd</sup> generation fabrics. However, these morphologies can only superficially analyse the external folding damage of SiC fibre braided fabrics, and more in-depth tests are needed to compare and explore the folding endurance of SiC fibres.

Figure 6 shows the folding endurance values of SiC fibre braided fabrics with different folding angles recorded by the reverse bend tester. The folding angle



**Figure 5. Surface morphologies of a) 2<sup>nd</sup> generation and b) 3<sup>rd</sup> generation [42] SiC fibre braided fabrics under varied folding conditions for comparative analysis**



**Figure 6. Folding endurance analyses for 2<sup>nd</sup> generation of SiC fibre braided fabrics, enabling a comparative assessment of their performance**

(+180°, -0°) indicated that the fabric sample was folded in half, and the folding angle (+180°, -180°) suggested that the fabric sample was doubly folded. Apparently, the damage caused by the reciprocating folding was greater than the single folding movement. Indeed, the folding endurance values measured under the condition of double fold were less than that under the condition of single fold, and all SiC fibre fabrics followed this behaviour. Under the condition of double fold, the outer

appearances of the 2<sup>nd</sup> generation SiC fibre fabrics after the different number of folds were photographed, as seen in Fig. 7. It can be seen from Figs. 6 and 7 that the folding endurance values of the 2<sup>nd</sup> generation SiC fabrics with three braiding angles (38.3°, 40.4°, and 41.9°) decrease with the increase of the braiding angle. In the double fold process, the 2<sup>nd</sup> generation SiC fabrics with braiding angle 38.3° became visibly narrower after folding 300 times, the edge began to unglue after folding 400 times, the fabric edges on both sides were completely unglued and loosed after folding 700 times, and the fabrics were broken after folding 1317 times. The fabrics with a braiding angle 40.4° became visibly narrower and the edge began to unglue after folding 280 times; the fabric edges on both sides were completely unglued and loosed after folding 450 times, and the fabrics were broken after folding 847 times. The fabrics with braiding angle 41.9° became visibly narrower and the edge began to unglue after folding 200 times; the fabric edges on both sides were completely unglued and loosed after folding 370 times, and the fabrics were broken after folding 757 times. In the previous study [42], we obtained the folding endurance values of the 3<sup>rd</sup> generation SiC fabrics, as seen in Fig. 8. The 2<sup>nd</sup> generation SiC fabrics had lower folding endurance values than the 3<sup>rd</sup> generation in general. Analysis of the folding life test results for both 2<sup>nd</sup> and 3<sup>rd</sup> generation SiC fibre fabrics reveal an interesting trend. As the braiding angle for the 3<sup>rd</sup> generation SiC fibre fabrics increases

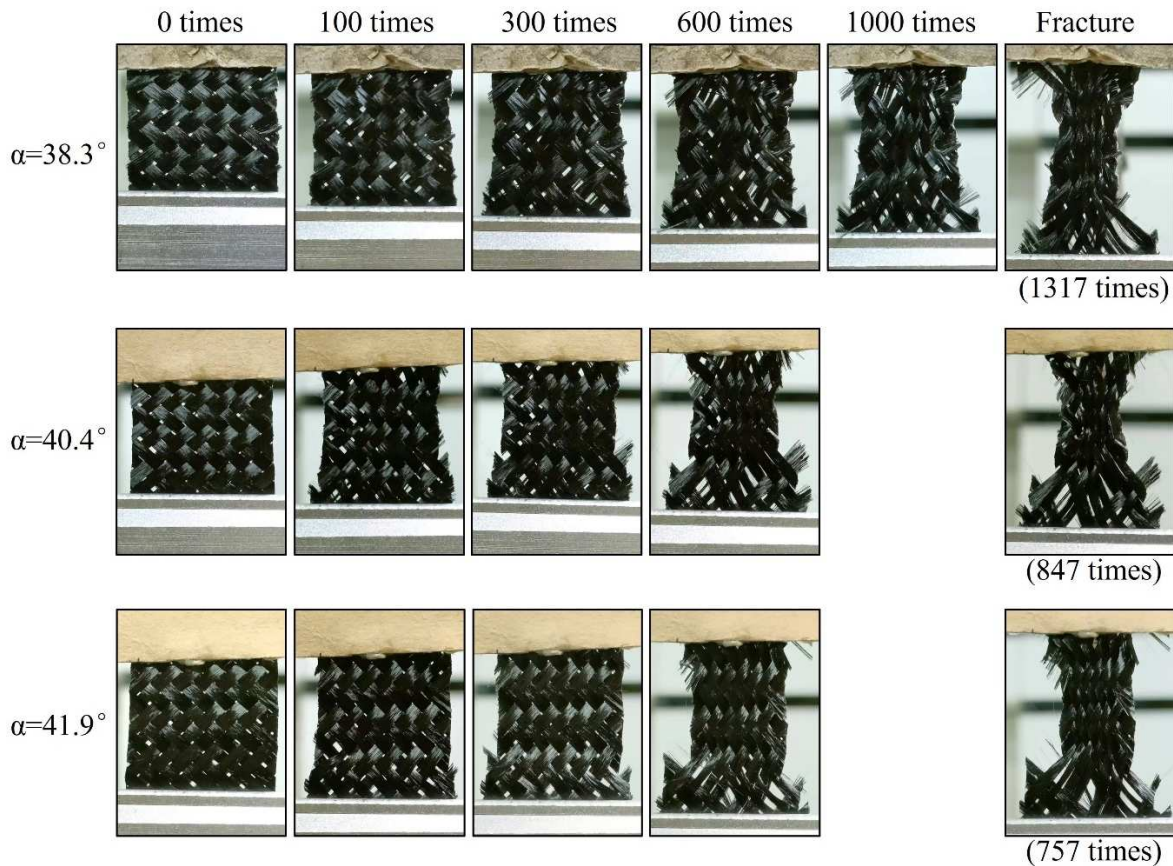


**Figure 7. Visual assessment of 2<sup>nd</sup> generation SiC fibre braided fabrics under double fold condition**



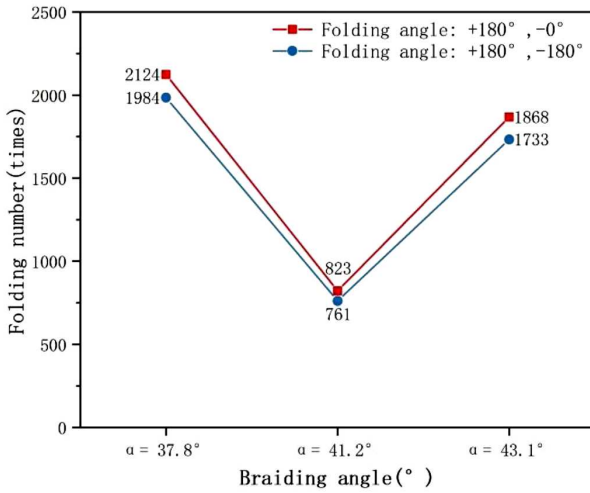


Figure 8. Folding endurance analyses for 3<sup>rd</sup> generation of SiC fibre braided fabrics [42]

within the range of 37.8° to 43.1°, the folding endurance values initially decrease before exhibiting an upward trend. Notably, for the 2<sup>nd</sup> generation SiC fibre fabrics, this trend is predominantly characterized by a decrease, ranging from 38.3° to 41.9°. Remarkably, within the specific braiding angle range of 41° to 42°, the SiC fibre fabrics exhibit their lowest folding endurance values, signifying their reduced resistance to repetitive bending and folding stresses.

In combination with Table 1 and Table 2 in Section 2, it can be seen that when the drafting speed has remained constant, the faster the braiding speed, the greater the braiding angle and tightness of the corresponding braided fabric. The folding line followed the axial braiding direction, so in the range of braiding angle from 37.8° to 43.1°, the larger the braiding angle, the less the folded parts of each fibre tow in fabric and the more the fibre tow interlaced parts in the unit area. For the fabric with smaller braiding angles, the interlaced friction actions between fibre tows were lower and mainly affected by the folding behaviours. When the number of folds was small, the functions of folding load were dominant, and the comprehensive effects of internal interlaced abrasion and external folding damage were growing. For the fabrics with medium range braiding angles, the influences of interlaced abrasion

behaviours between fibre tows were more pronounced than that of fabrics with smaller angles, and the consequences of folding actions were greater than that of fabrics with larger angles, so they had the lowest folding endurance values and the fastest folding damage process.

### 3.2. Folding endurance and damage characteristics

In order to deeply characterize and analyse the folding damage mechanisms of SiC fibres, the mechanical properties of the 2<sup>nd</sup> and 3<sup>rd</sup> generation SiC fibre tows and their fabrics before and after folding were further studied.

#### Mechanical properties of SiC fibre tows

The strength-strain curves were calculated and plotted using the displacement, load and other experimental data obtained from the tensile test of fibre tows, as shown in Fig. 9. The average tensile breaking force, breaking strength and elongation at break of the original 2<sup>nd</sup> generation SiC fibre tows were 183.42 N, 0.5917 N/tex and 2.670%, respectively. The average tensile breaking force, breaking strength, and elongation at break of the original 3<sup>rd</sup> generation SiC fibre tows were 65.85 N, 0.3618 N/tex, and 1.443%, respectively [42]. All curves' trends were consistent and aligned with the original brittle fracture characteristics of SiC fibre tows. The breaking strengths of the 2<sup>nd</sup> generation SiC fibre tows were generally greater than that of the 3<sup>rd</sup> generation because the oxygen contents of the 3<sup>rd</sup> generation SiC were low. Figures 9b,c show the strength-strain curves of the original SiC fibre tows and the tows in fabric with different braiding angles before folding. This is equivalent to discussing the effects of the braiding process on the tensile properties of SiC fibre tows. The tensile strengths of SiC tows after braiding and before folding decreased compared with that of original fibre tows, and both the 2<sup>nd</sup> and 3<sup>rd</sup> generation SiC followed the trend. Figures 10 and 11 show the tensile breaking forces and force loss rates of SiC fibre tows disassembled from fabrics with different braiding angles under different folding conditions.

It can be seen from Figs. 9, 10 and 11 that the tensile breaking forces of the 2<sup>nd</sup> and 3<sup>rd</sup> generation SiC fibre tows decrease with the increasing number of folds and

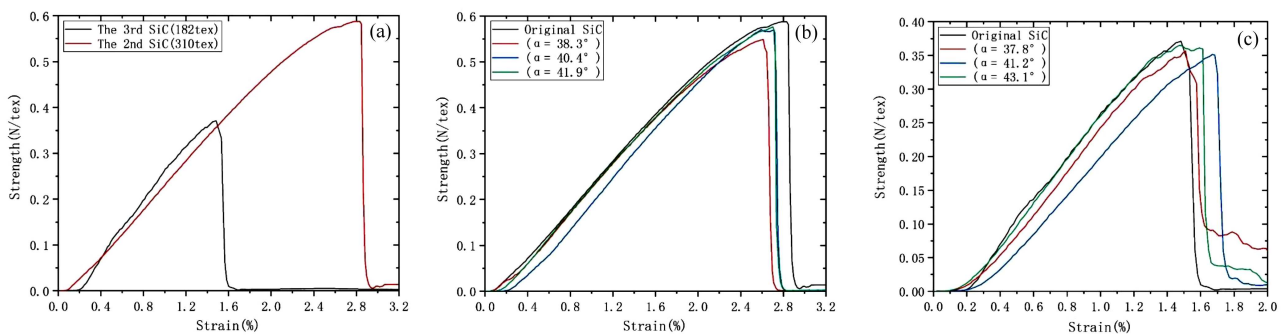


Figure 9. Comparison of the strength-strain curves between 2<sup>nd</sup> and 3<sup>rd</sup> generation SiC fibre tows (a), the strength-strain curve for 2<sup>nd</sup> generation (b) and 3<sup>rd</sup> generation [42] SiC fibre tows (c)

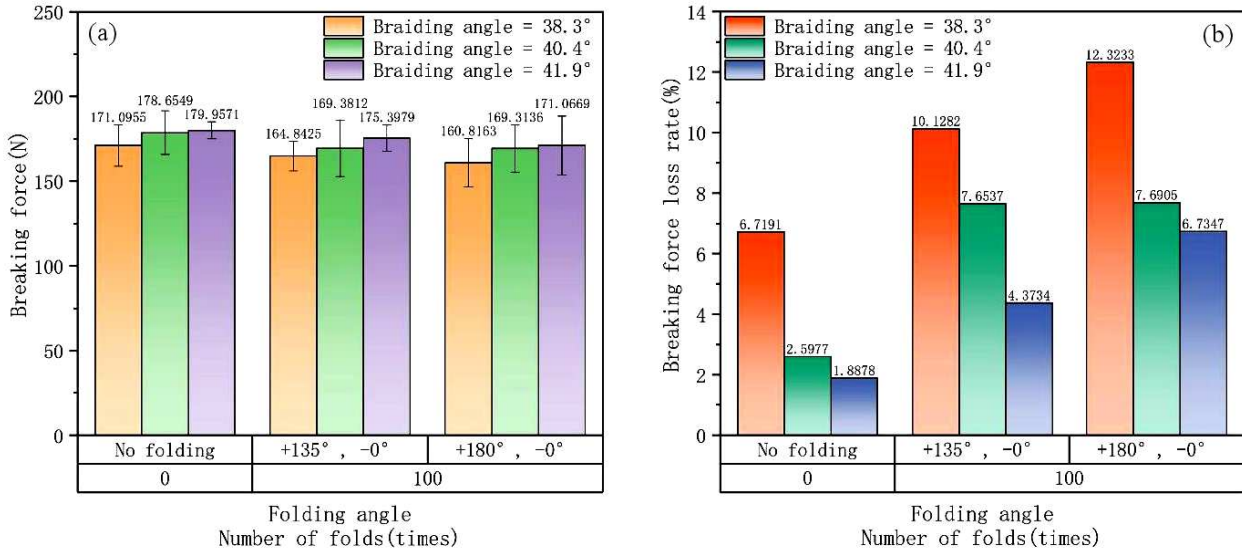


Figure 10. Tensile breaking forces and force loss rates of the 2<sup>nd</sup> generation SiC fibre tows

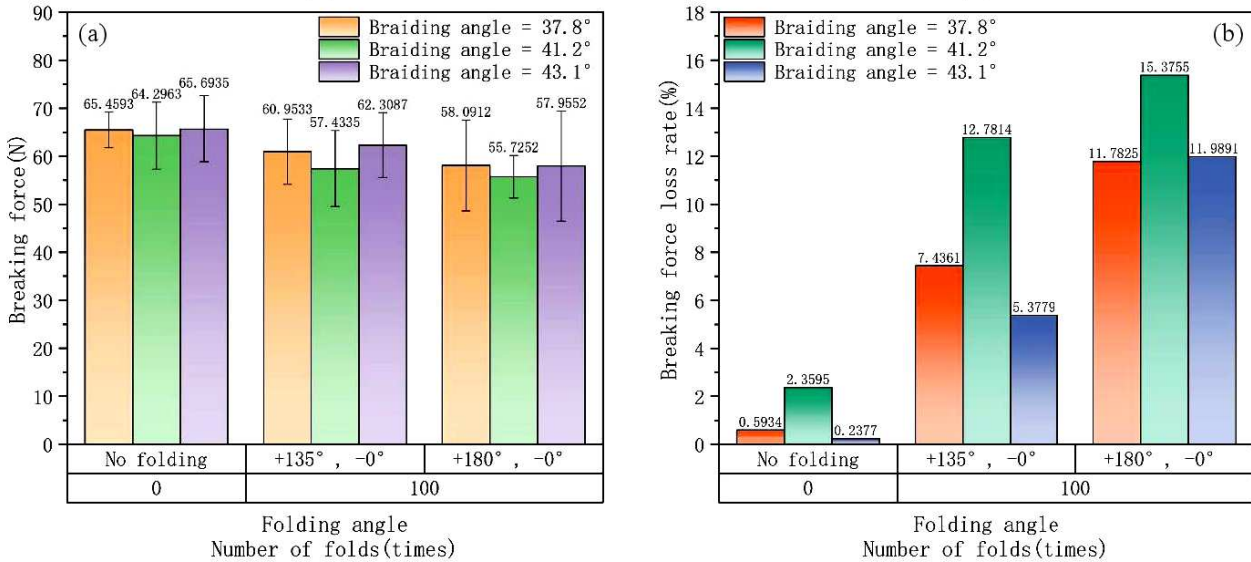


Figure 11. Tensile breaking forces and force loss rates of the 3<sup>rd</sup> generation SiC fibres tows [42]

folding angles. In other words, the greater the number of folds and folding angles, the greater the force loss rates of fibre tows. The force loss rates of the 2<sup>nd</sup> generation SiC fibre tows were slightly lower than that of the 3<sup>rd</sup> generation SiC in general, corresponding to the optical microscope surface morphology results in Section 3.1. The 2<sup>nd</sup> generation SiC fabrics were arranged neatly, and the displacements and deformations of their tows during folding were less than that of the 3<sup>rd</sup> generation fabrics. Hence, the force losses were slightly lower. For the 2<sup>nd</sup> generation SiC fabrics with three braiding angles (38.3°, 40.4° and 41.9°), the force loss rates of SiC fibre tows decreased with the increase of braiding angle. For the 3<sup>rd</sup> generation SiC fabrics with three braiding angles (37.8°, 41.2° and 43.1°), the force loss rates of SiC fibre tows increased at first and then decreased with the increased braiding angle. Combined with the tensile properties results of the 2<sup>nd</sup> and 3<sup>rd</sup> generation SiC

fibre tows, it is found that the force loss rates of SiC fibre tows increased at first and then decreased when the braiding angle was raised from 37.8° to 43.1°. There should be a critical point roughly in the interval near the braiding angle of 37.8° to 38.3°, where the tensile breaking force loss rates of SiC fibre tows are the greatest. It had been stated in Section 3.1 that a fabric with a larger braiding angle had a larger tightness. The folded parts of each fibre tow depended on the braiding angle, and the interlaced abrasion parts of fibre tows in the unit area depended on the areal density. The fibre tows in fabric with a small braiding angle had more folded parts and less interlaced parts. The fibre tows in fabric with a large braiding angle had less folded parts and more interlaced parts. For the inner fibre tows of fabric with a medium braiding angle, the interlaced abrasions were more than that of the fabric with a small braiding angle, and the folding damages were more than that of the fabric with

a large braiding angle. When the number of folds was small, the fibre tows were mainly affected by folding load and the effects of interlaced abrasions were low. The comprehensive results of interlaced abrasion and folding force became increasingly apparent with the increasing number of folds. At the same time, interleaved wear would also imperceptibly act on and accelerate the damage evolution process of fabrics. Therefore, the folding lives of the fabrics with medium braiding angles were shorter, and the force losses of their fibre tows were higher.

*Mechanical properties of SiC fabrics*

The stress-strain curves were calculated and plotted by using the displacement, load and other experimental data obtained from the fabric tensile test, as shown in Fig. 12. Figure 12b indicates the typical stress-strain curves of the 2<sup>nd</sup> generation SiC fabrics with three braiding angles before folding. Since the fibre tows in fabrics had different fracture times caused by uneven forces during stretching, all curves showed drastic fluctuations. The tensile breaking forces and force loss rates of SiC fabrics with different braiding angles under different

folding conditions are shown in Figs. 13 and 14. The average tensile breaking forces, breaking strengths and elongations at break of the 2<sup>nd</sup> generation SiC fibre fabrics before folding were listed in Table 4, and the tensile property data of the 3<sup>rd</sup> generation SiC fabrics obtained in the previous study [42] were also included.

As it can be seen from Figs. 12, 13 and 14 as well as in Table 4, the breaking strengths of the 2<sup>nd</sup> generation SiC fibre fabrics were generally lower than that of the 3<sup>rd</sup> generation fabrics because the fineness of the 2<sup>nd</sup> generation SiC was thicker and the number of fibre tows per unit area of fabrics were lower. Clearly, with the increased number of folds and folding angles, the tensile breaking strengths of the 2<sup>nd</sup> and 3<sup>rd</sup> generation SiC fabrics became lower and the fabric strength losses became greater. The tensile breaking forces of the same SiC fibre fabrics increased with the increase of braiding angle, because the load of the fabric tensile test was along the radial braiding direction, and the direction of fibre tows in fabric with the small braiding angle was farther away from the radial direction. The force loss rates of the same SiC fabrics decreased at first and then increased with the increase of braiding angle,

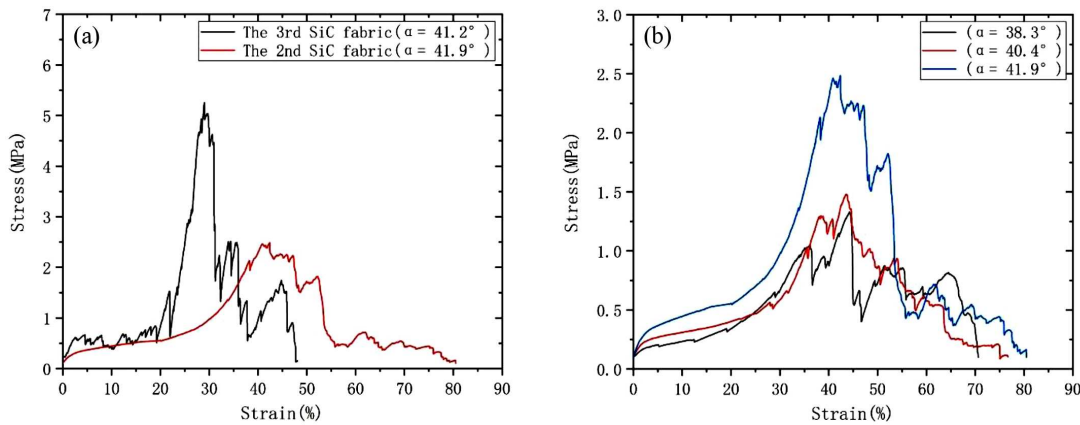


Figure 12. Comparison of the stress-strain curves between 2<sup>nd</sup> and 3<sup>rd</sup> generation SiC fibre fabrics (a) and the stress-strain curve for 2<sup>nd</sup> generation SiC fibre fabrics before undergoing folding tests (b)

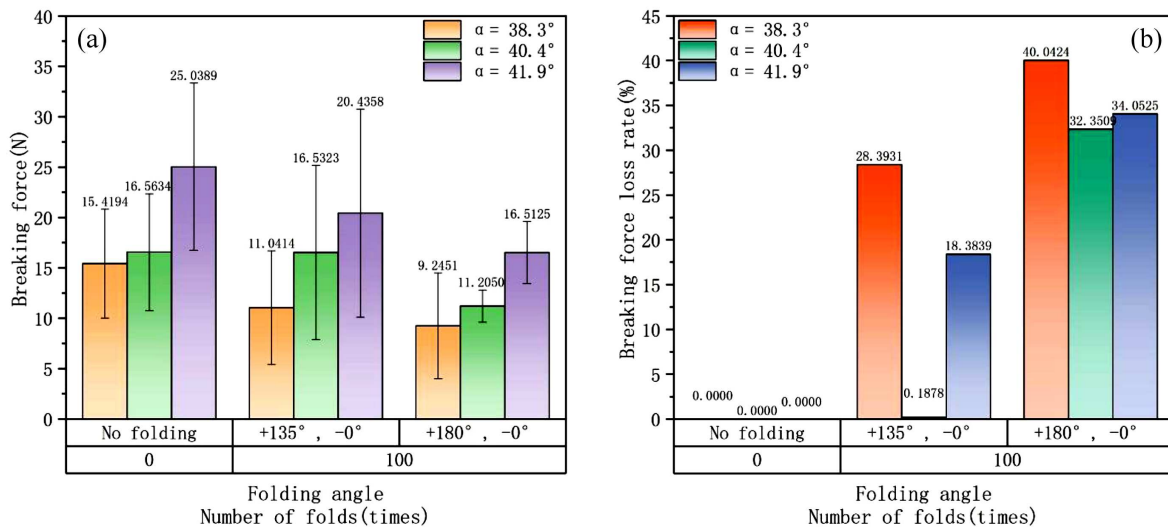


Figure 13. The tensile breaking forces (a) and the force loss rates (b) of the 2<sup>nd</sup> generation SiC fabrics



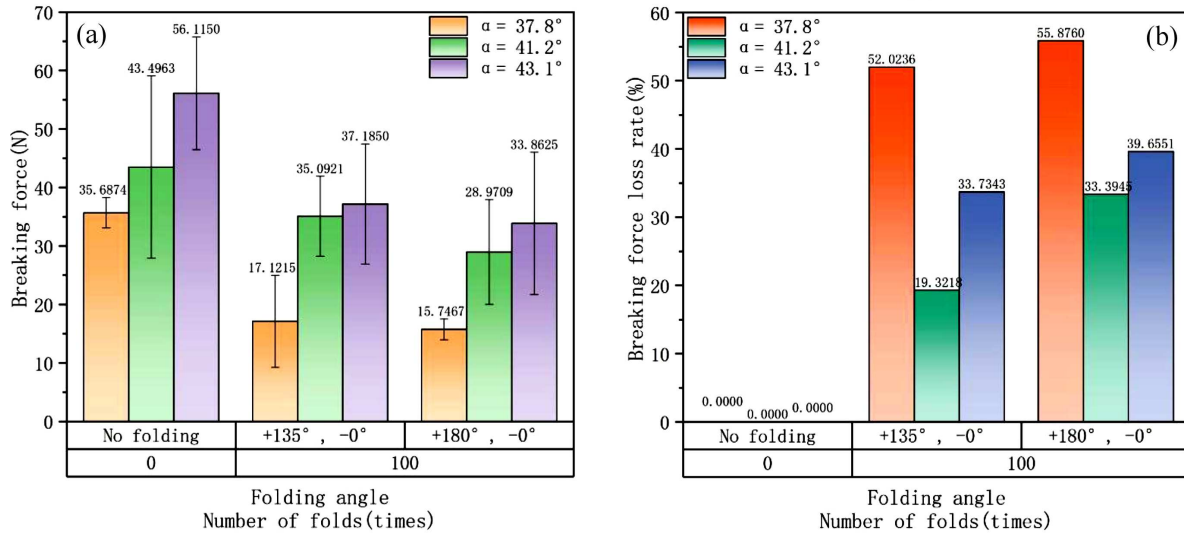


Figure 14. The tensile breaking forces (a) and the force loss rates (b) of the 3<sup>rd</sup> generation SiC fabrics [42]

Table 4. Tensile properties of SiC fibre braided fabrics before folding

Fabric	Braiding angle [°]	Breaking force [N]	Breaking strength [MPa]	Elongation at break [%]
The 2 <sup>nd</sup> generation SiC fibre fabric	38.3	15.42	1.590	44.78
	40.4	16.56	1.721	42.13
	41.9	25.04	2.510	40.38
The 3 <sup>rd</sup> generation SiC fibre fabric [42]	37.8	35.69	3.911	43.72
	41.2	43.50	4.874	26.15
	43.1	56.12	5.876	35.99

which were the trends for both the 2<sup>nd</sup> and 3<sup>rd</sup> generation fabrics. When the number of folds was small, the folding force mainly damaged the fabrics and the interlaced abrasion actions on the fabric level were low. In addition, the strength losses of the 2<sup>nd</sup> generation SiC fabrics were generally lower than those of the 3<sup>rd</sup> generation fabrics. It should be taken into account that the small fabric sample sizes may produce the edge effects and affect the references of fabric mechanical properties test results.

#### IV. Conclusions

This study used the 2<sup>nd</sup> and 3<sup>rd</sup> generation continuous SiC fibres to fabricate 2D biaxial braided fabrics with varying braiding angles. Subsequently, a series of tests, including repeated folding tests, optical microscope measurements and tensile tests, were carried out. Finally, the effects of the braiding process, braiding angle, number of folds and folding angle on the folding endurance and damage mechanisms of SiC fibres were compared and discussed.

Repeated folding tests showed that the surfaces of SiC fabrics after folding exhibited phenomena such as fuzzing, snagging and local filament breakage. Moreover, with an increasing number of folds, the arrangement of fibre tows became more disordered. Additionally, when the number of folds was less than 100 times, the surface abrasion conditions were more subtle in the

2<sup>nd</sup> generation SiC fabrics than those in the 3<sup>rd</sup> generation. Furthermore, although the folding lives of the 2<sup>nd</sup> generation SiC fabrics were slightly lower than those of the 3<sup>rd</sup> generation fabrics, within a braiding angle range from 37.8° to 43.1°, it was determined that SiC fibre fabrics with a braiding angle between 41° and 42° exhibited the lowest resistance to repeated folding.

According to the tensile test results of fibre tows, the 2<sup>nd</sup> generation SiC exhibited higher breaking strengths and lower force loss rates compared to the 3<sup>rd</sup> generation SiC. The mechanical properties of SiC fibre tows decreased due to the braiding process, increased number of folds and larger folding angles causing the greatest strength losses in within a braiding angle range from 37.8° to 43.1°. Beyond an angle of 38.3°, there was a gradual decrease in force loss rates for SiC fibre tows with increasing braiding angle.

According to the tensile test results of fabrics, in comparison with the 3<sup>rd</sup> generation SiC fabrics, the 2<sup>nd</sup> generation SiC fabrics exhibited lower breaking strengths and force loss rates. The tensile breaking forces of SiC fibre fabrics were found to be influenced by both the number of folds and the folding angle. The SiC fabrics with larger braiding angles demonstrated higher tensile breaking forces. The strength losses of the 2<sup>nd</sup> and 3<sup>rd</sup> generation fabrics initially decreased and then increased with an increase in braiding angle. However, it should be noted that edge effects may impact the referable significance of mechanical results for smaller-sized fabrics.

From the perspective of fibre tows, the 2<sup>nd</sup> generation SiC fibre tows exhibited superior resistance to the repeated folding compared to the 3<sup>rd</sup> generation. Regarding folding life, the 3<sup>rd</sup> generation SiC fibre fabrics demonstrated a higher number of folding endurance values than their 2<sup>nd</sup> generation counterparts. Based on various experimental results, it was observed that the SiC fibres in fabrics with large braiding angles displayed exceptional folding endurance. The present findings suggest that the mechanical properties of SiC fibres are influenced by both the textile forming process and the usage process (repeated folding process), resulting in consequential damage. Therefore, optimizing structural parameters and coating fibre tows can enhance the folding endurance of SiC fibres and their fabrics, respectively, addressing both processing and utilization perspectives to enable their application in flexible, foldable thermal protection materials. Regarding the work presented in this article, our investigation is limited to a slightly narrow range of braiding angles. Future research will primarily examine internal damage and simulating force conditions experienced by fibre tows during folding.

**Acknowledgement:** The work was financially supported by Science and Technology on Advanced Ceramic Fibres and Composites Laboratory, National University of Defense Technology.

## References

- O. Uyanna, H. Najafi, “Thermal protection systems for space vehicles: A review on technology development, current challenges and future prospects”, *Acta Astronautica*, **176** (2020) 341–356.
- H. Huang, L. Su, C. Lei, J. Li, E. Zhang, W. Li, J. Yang, Y. Zhao, Y. Pei, H. Zhang, “Reusable thermal protective materials: application and research progress”, *Acta Aeronautica et Astronautica Sinica*, **41** [12] (2020) 6–40.
- Y. Takahashi, T. Koike, N. Oshima, K. Yamada, “Aerothermodynamic analysis for deformed membrane of inflatable aeroshell in orbital reentry mission”, *Aerospace Sci. Technol.*, **92** (2019) 858–868.
- J. Guo, G. Lin, J. Zhang, X. Bu, H. Li, “Hypersonic aerodynamics of a deformed aeroshell in continuum and near-continuum regimes”, *Aerospace Sci. Technol.*, **93** (2019) 105296.
- Y. Takahashi, T. Ohashi, N. Oshima, Y. Nagata, K. Yamada, “Aerodynamic instability of an inflatable aeroshell in suborbital re-entry”, *Phys. Fluids*, **32** (2020) 075114.
- V. Carandente, R. Savino, V. D’Orlando, R. Fortezza, “A study on earth Re-entry capsules with deployable aerobrakes for recoverable microgravity experiments”, *Microgravity Sci. Technol.*, **27** [3] (2015) 181–191.
- G. Zuppari, R. Savino, G. Mongelluzzo, “Aero-thermodynamic analysis of a low ballistic coefficient deployable capsule in Earth re-entry”, *Acta Astronautica*, **127** (2016) 596–692.
- S. Mungiguerra, G. Zuppari, R. Savino, “Rarefied aerodynamics of a deployable re-entry capsule”, *Aerospace Sci. Technol.*, **69** (2017) 395–403.
- D.D. Johnson, “Nextel 312 ceramic fiber from 3M”, *J. Industrial Textiles*, **11** (1982) 282–296.
- D. Li, B. Li, Y. Zheng, S. Gao, “On the mechanical, thermophysical and dielectric properties of Nextel™ 440 fiber reinforced nitride matrix (N440/Nitride) composites”, *Ceram. Int.*, **44** [6] (2018) 6137–6143.
- S. Hughes, J. Ware, J. Del Corso, R. Lugo, “Deployable aeroshell flexible thermal protection system testing”, *20<sup>th</sup> AIAA Aerodynamic Decelerator Systems Technology Conference and Seminar*, 2009.
- H. Wright, A. Cutright, J. Corliss, “HEART fight test overview”, *9<sup>th</sup> International Planetary Probe Workshop*, 2012.
- R. Wu, P. Roberts, C. Soutis, C. Dive, “Flexible heat shields deployed by centrifugal force”, *Acta Astronautica*, **152** (2018) 78–87.
- R. Wu, P. Roberts, C. Soutis, C. Dive, “Downrange manoeuvre and oscillation suppression of a self-regulating centrifugally deployed flexible heat shield using a controlled reaction wheel”, *Acta Astronautica*, **161** [2] (2019) 415–424.
- R. Wu, P. Roberts, L. Xu, C. Soutis, C. Dive, “Deployable self-regulating centrifugally-stiffened decelerator (DESCENT): Design scalability and low altitude drop test”, *Aerospace Sci. Technol.*, **114** (2021) 106710.
- G. Zhang, Y. Xue, P. Liu, A. Guo, H. Du, L. Yan, J. Liu, “High emissivity double-layer coating on the flexible aluminum silicate fiber fabric with enhanced interfacial bonding strength and high temperature resistance”, *J. Eur. Ceram. Soc.*, **41** [2] (2020) 1452–1458.
- D. Gosset, A. Jankowiak, T. Vandenberghe, M. Maxel, C. Colin, N. Lochet, L. Luneville, “Effect of high temperature heat treatment on the microstructure and mechanical properties of third generation SiC fibers”, *MRS Proceedings*, **1514** [1] (2013) 131–137.
- S. Cao, J. Wang, H. Wang, “Formation mechanism of large SiC grains on SiC fiber surfaces during heat treatment”, *CrystEngComm*, **18** [20] (2016) 3674–3682.
- W. Guo, S. Xin, W. Hu, Y. Gao, “Study on damage performance of silicon carbide fiber bundles in braiding process”, *J. Textile Res.*, **43** [12] (2022) 69–74.
- L. Li, K. Jian, Y.F. Wang, “The effect of heat treatment on the microstructure and mechanical properties of KD-II SiC fibers in air”, *Key Eng. Mater.*, **726** (2017) 132–136.
- C. Wu, Q. Chen, Y. Zhang, Y. Gou, Y. Wang, H. Wang, J. Chen, “Study on fine microstructure and properties of two typical continuous SiC fibers”, *J. Hunan University (Natural Sci.)*, **46** [12] (2019) 71–78.
- C. Yang, J. Wu, A. Ditta, L. Wei, “Effects of temperature and atmosphere on microstructural evolution and mechanical properties of KD-II SiC fibers”, *Ceram. Int.*, **46** [15] (2020) 24424–24434.
- W. Guo, Y.T. Gao, W. Hu, X. Wu, “Study on the mechanical property of high-performance silicon carbide fiber”, *Adv. Eng. Mater.*, **24** [7] (2022) 2101407.
- H. Pi, Y. Wang, “Effect of high temperature heat treatment on properties of domestic second-generation SiC fiber”, *J. Harbin Inst. Technol.*, **54** (2022) 43–48.
- S. Wu, Y. Gou, Y. Wang, Q. Song, Q. Zhang, Y. Wang, “Effect of heat treatment on composition, microstructure and mechanical property of domestic KD-SA SiC fibers”, *J. Inorganic Mater.*, **38** [5] (2023) 569–576 (in Chinese).
- L. Li, K. Jian, Y. Wang, “Study of oxidation resistance of KD-I and KD-II continuous SiC fibers in air”, *Mater. Rev.*

- 30 (2016) 308–312.
27. D. Gosset, C. Colin, A. Jankowiak, T. Vandenberghe, N. Lochet, “X-ray diffraction study of the effect of high-temperature heat treatment on the microstructural stability of third-generation SiC fibers”, *J. Am. Ceram. Soc.*, **96** [5] (2013) 1622–1628.
  28. L. Li, K. Jian, X. Mao, Y. Wang, “Wet oxidation behavior of near-stoichiometric SiC fibers in the simulated aeroengine circumstance”, *Int. J. Corrosion*, **2018** (2018) 4319354.
  29. D. Ding, F. Lou, Y. Shi, J. Chen, “Influence of thermal oxidation on complex permittivity and microwave absorbing potential of KD-I SiC fiber fabrics”, *J. Eng. Fibers Fabrics*, **9** [2] (2014) 99–104.
  30. P. Wang, F. Liu, H. Wang, H. Li, Y. Gou, “A review of third generation SiC fibers and SiC<sub>f</sub>/SiC composites”, *J. Mater. Sci. Technol.*, **35** [12] (2019) 2743–2750.
  31. M. Zu, S.M. Zou, S. Han, H.T. Liu, “Effects of heat treatment on the microstructures and properties of KD-I SiC fibres”, *Mater. Res. Innovations*, **19** [sup1] (2015) 437–441.
  32. S. Cao, J. Wang, H. Wang, “Effect of heat treatment on the microstructure and tensile strength of KD-II SiC fibers”, *Mater. Sci. Eng. A*, **673** (2016) 55–62.
  33. Y. Gan, X. Wang, J. Wang, H. Wang, “Preparation and characterization of near-stoichiometric silicon carbon fibres”, *RSC Advances*, **8** [31] (2018) 17453–17461.
  34. Y. Gou, H. Wang, K. Jian, C. Shao, X. Wang, “Preparation and characterization of SiC fibers with diverse electrical resistivity through pyrolysis under reactive atmospheres”, *J. Eur. Ceram. Soc.*, **37** [2] (2017) 517–522.
  35. W. Bai, K. Jian, “The microstructure and electrical resistivity of near-stoichiometric SiC fiber”, *IOP Conference Series: Mater. Sci. Eng.*, **490** [2] (2019) 022057.
  36. Z. Su, L. Zhang, Y. Li, S. Li, L. Chen, “Rapid preparation of SiC fibers using a curing route of electron irradiation in a low oxygen concentration atmosphere”, *J. Am. Ceram. Soc.*, **98** [7] (2015) 2014–2017.
  37. G. Zhang, Y. Wu, C. Liu, X. Luo, “Study on the preparation of near-stoichiometric SiC fibers by controlling pyrolysis atmosphere”, *J. Xiamen University (Natural Sci.)*, **45** [5] (2006) 683–687 (in Chinese).
  38. X. Tang, L. Zhang, H. Tu, H. Gu, L. Chen, “Decarbonization mechanisms of polycarbosilane during pyrolysis in hydrogen for preparation of silicon carbide fibers”, *J. Mater. Sci.*, **45** [21] (2010) 5749–5755.
  39. China National Light Industry Council, “Paper and board-Determination of folding endurance”, *GB/T 457-2008.2008-08-19 Standard* (in Chinese).
  40. China Aerospace Science and Technology Corporation, “Test methods for continuous silicon carbide fiber - Part 4: Tensile properties of filament yarn”, *GB/T 34520.4-2017.2017-11-01 Standard* (in Chinese).
  41. China National Textile and Apparel Council, “Test method for tensile properties of 3D braided fabric and its polymer matrix composites”, *GB/T 33613-2017.2017-05-12 Standard* (in Chinese).
  42. Q. Li, Y. Gao, W. Hu, “Folding endurance and damage mechanisms of SiC fiber braided fabrics”, *Ceram. Int.*, **49** (2023) 38339–38350.